



Molecular Crystals and Liquid Crystals

Publication details, including instructions for authors and subscription information:

<http://www.tandfonline.com/loi/gmcl16>

Temperature Dependent Electron Trapping in Anthracene

K. E. Meyer^{a, c}, L. B. Schein^{a, d}, R. W. Anderson^a,
R. S. Narang^a & A. R. Mcghie^b

^a Xerox Corporation, Webster Research Center,
W-114, Rochester, New York, 14644

^b Laboratory for Research on the Structure of
Matter, University of Pennsylvania, Philadelphia,
Pennsylvania, 19104

^c Dept. of Physics and Astronomy, University of
Rochester, Rochester, New York, 14620

^d IBM Research Laboratory, K461282, 5600 Cottle
Rd., San Jose, CA, 95193

Version of record first published: 20 Apr 2011.

To cite this article: K. E. Meyer, L. B. Schein, R. W. Anderson, R. S. Narang & A. R. Mcghie (1983): Temperature Dependent Electron Trapping in Anthracene, *Molecular Crystals and Liquid Crystals*, 101:3-4, 199-218

To link to this article: <http://dx.doi.org/10.1080/01406568308072529>

PLEASE SCROLL DOWN FOR ARTICLE

Full terms and conditions of use: <http://www.tandfonline.com/page/terms-and-conditions>

This article may be used for research, teaching, and private study purposes. Any substantial or systematic reproduction, redistribution, reselling, loan,

sub-licensing, systematic supply, or distribution in any form to anyone is expressly forbidden.

The publisher does not give any warranty express or implied or make any representation that the contents will be complete or accurate or up to date. The accuracy of any instructions, formulae, and drug doses should be independently verified with primary sources. The publisher shall not be liable for any loss, actions, claims, proceedings, demand, or costs or damages whatsoever or howsoever caused arising directly or indirectly in connection with or arising out of the use of this material.

Temperature Dependent Electron Trapping in Anthracene

K. E. MEYER,[†] L. B. SCHEIN,[‡] R. W. ANDERSON and R. S. NARANG

*Xerox Corporation, Webster Research Center, W-114, Rochester,
New York 14644*

and

A. R. MCGHIE

*Laboratory for Research on the Structure of Matter, University of Pennsylvania,
Philadelphia, Pennsylvania 19104*

(Received June 20, 1983)

We present data for the electron trapping lifetime measured in the c' direction of anthracene over a wide range of temperatures (81–374 K) and applied electric fields (0.10–4.73 V/ μm). Over these ranges the lifetime is activated and the activation energy is independent of the field. We have considered several trapping models. Only one of these, a model consisting of a deep trap level and associated shallow “pre-trap” level, can adequately account for our data. We discuss briefly the possibility of a temperature dependent trapping cross-section.

I. INTRODUCTION

In transient photoconductivity (TPC) experiments it has been observed that the apparent electron trapping lifetime decreases rapidly with decreasing temperature. This effect has been well-known, but to the authors' knowledge, has only been briefly mentioned in three papers (refs. 1, 2, and 6). The decay is so fast at low temperatures that an important feature, the transit time, which is used to calculate the

[†]Present Address: Dept. of Physics and Astronomy, University of Rochester, Rochester, New York 14620.

[‡]Present Address: IBM Research Laboratory K461282, 5600 Cottle Rd., San Jose, CA 95193.

carrier mobility, is obscured. The effect determines the lowest temperature at which a mobility may be determined (31 K in naphthalene¹ and 78 K in anthracene²). Understanding this trapping effect may allow mobility measurements to be extended to lower temperatures. This is particularly important in anthracene, where a band-to-hopping transition is expected analogous to that which has already been observed in naphthalene.¹

Understanding the temperature dependence of the charge carrier trapping lifetime is also important in its own right, as both the theoretical understanding of trapping mechanisms and the experimental techniques used for trap characterization in high-purity molecular crystals are incomplete at best. From a practical point of view, traps can limit the speed and efficiency of devices incorporating organic materials (e.g., electroluminescence devices^{3,4}).

While TPC experiments have been used extensively to measure carrier mobilities,⁵ in some cases⁶⁻¹⁰ molecular crystals have been doped with a particular impurity to study how that impurity acts as a trap. Sometimes the transport becomes trap limited, resulting in an *effective* electron or hole mobility which is activated with temperature. Analysis of the mobility data yields trap depths and concentrations. Traps that limit the transport in this way are referred to as shallow traps, and the corresponding mobility is labeled shallow trap controlled mobility. Sometimes the mobility remains unaffected, but the charge carriers exhibit a reduced lifetime. These are called “deep” traps; they have been studied to a much smaller extent with the TPC experiment. Surface roughening has been found to introduce shallow hole traps and deep electron traps.¹¹ Mechanically induced dislocations have no effect on hole transport but do act as deep electron traps.¹²

Two other experimental techniques, thermally stimulated currents (TSC) and space charge limited currents (SCLC), have been applied to the problem of trap characterization in molecular crystals. The two techniques have been used together to study deep hole traps in pure anthracene.^{13,14} TSC experiments have also revealed deep hole traps,¹⁵ shallow hole traps,¹⁶ and both deep and shallow electron traps¹⁷ in pure and doped anthracene, and deep electron traps induced by surface photo-oxidation.¹⁸ SCLC experiments have shown evidence of bulk hole traps with a distribution of trap depths in pure anthracene.¹⁹ Current understanding of trapping processes relies heavily on the theoretical work of Silinsh,²⁰ Sworakowski,²¹ and a few others.^{22,23}

It is the purpose of this paper to present a detailed experimental and theoretical study of the behavior of “deep” traps in molecular

crystals using TPC measurements. After discussing experimental details in Section II, our results of the electron trapping lifetime in anthracene as a function of temperature and applied electric field are presented in Section III. In Section IV the predictions of several existing trapping models are compared with our results and we present our conclusions in Section V.

II. EXPERIMENT

The experiment that has been performed is the transient photoconductivity experiment, which has been well-established as a tool for determining charge-carrier mobilities in organic crystals (a complete list of references for molecular crystals is given in Ref. 5). The anthracene crystals used were grown with the Bridgman technique and zone-refined for high purity. Individual samples were cleaved parallel to the *ab* plane to the desired thickness (100–500 μm). Typical cross-sectional areas were 0.05–0.5 cm^2 . The samples were mounted with one face pressed against Nesa-coated quartz (the front electrode), the other surface having been painted with silver paint. A brass plunger made electrical contact between the silver paint and the detection electronics. A DC bias voltage (–50 to –2000 V) was applied to the front electrode and a Q-switched Nd-glass laser (FWHM ~ 20 nsec, frequency doubled twice to 2650 \AA , energy density ~ 1 mJ/cm^2) illuminated the front surface creating a sheet of free electrons. The drifting electrons induced a current which flowed across a load resistor to ground. The resulting voltage waveform was amplified (Comlinear Corp. #E103 high-bandwidth op-amp) and recorded on a Nicolet 2090 digital oscilloscope (maximum sampling rate 20 MHz).

Transient responses were recorded for a wide range of applied voltages and sample temperatures (temperature was controlled to ± 0.1 K by a Ransco SD14 nitrogen-flow temperature chamber). In all cases the response time of the electronics was much faster than the time scale of the experiment.

Several effects may be neglected in terms of their contribution to the decay time of the current (from which electron trapping lifetimes were obtained). We have determined that electron current injected by the silver paint is negligible for fields below ~ 8 $\text{V}/\mu\text{m}$. The Nesa-coated quartz is a more efficient injector of holes, creating a current density $J \sim 10^{-5}$ A/cm^2 at a field of 2 $\text{V}/\mu\text{m}$. This current density is two orders of magnitude smaller than the amplitude of our current transients and falls off rapidly with decreasing voltage.

Space charge effects occur when the self-induced field of the photo-generated charge is large enough to distort the externally applied field. The effects have three trademarks: i) the amplitude of the current transient becomes independent of the photon flux, ii) the shape of the transient is distorted in a well-known way,²⁴ and iii) the apparent transit time of the carriers is reduced. In all cases our experiment was performed well below the space-charge regime.

Finally, diffusion²⁵ of the charge sheet may be neglected. The effect of diffusion and other sources of dispersion of the charge sheet is to spread out the charge packet spatially and hence smear out the observed transit time, not significantly affecting the time-dependence of the current before the transit time.

III. RESULTS

Figure 1 shows a typical transient response. Also shown is an exponential fit to the data in the time-span indicated by the arrows. At times shorter than $\sim 4 \mu\text{sec}$ the current is nonexponential. If the response time for the circuit is made less than 20 nsec, then the leading edge of the current may be resolved into a current spike that follows

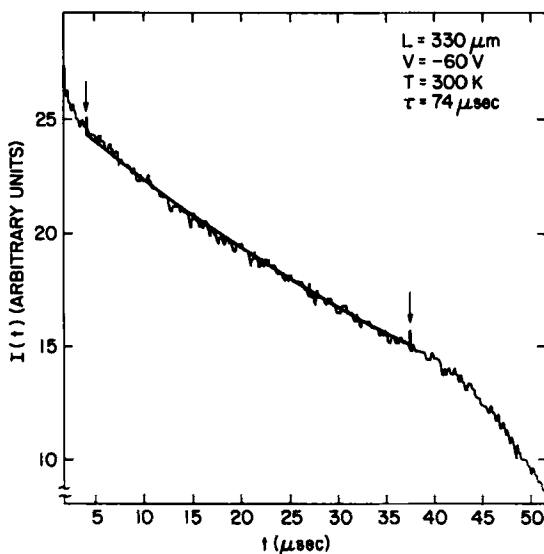


FIGURE 1 Typical electron transient response in anthracene. The heavy line is a fit of a pure exponential function to the data, with decay constant $\tau = 74 \mu\text{sec}$.

the laser pulse superimposed on the exponential decay. This current spike has been observed in the past²⁶ and its origins are not well understood.

The shoulder in the current at $\sim 47 \mu\text{sec}$ indicates the transit time. This feature is not sharp but somewhat rounded, which suggests that diffusion or other spatial dispersion of the charge sheet is occurring. For this reason data near the transit time have not been included in the exponential fits. The remaining feature, the long tail in the current beyond the transit time, which may reflect detrapping of trapped carriers from shallow traps, has been ignored in our analysis.

To test whether the current decayed to a steady-state (non-zero) value (a prediction of the shallow trap model, see below), the applied field was reduced. This increased the transit time and allowed longer

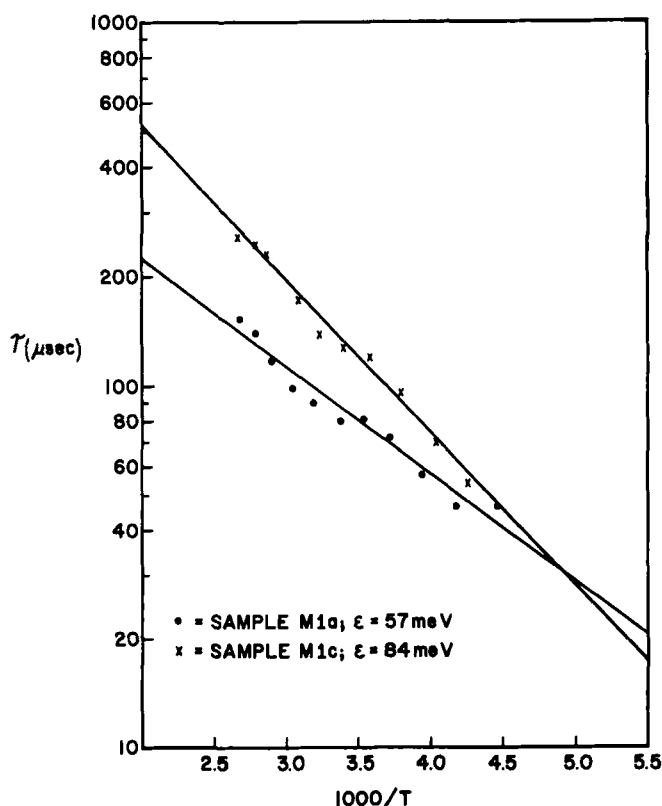


FIGURE 2 Electron trapping lifetime in anthracene (c' direction) versus inverse temperature for two samples from crystal M1, indicating the activated behavior. The applied field is $0.20 \text{ V}/\mu\text{m}$ for sample M1a and $0.18 \text{ V}/\mu\text{m}$ for sample M1c. ϵ is the activation energy.

time scales to be investigated. With very low fields and transit times of several msec, no steady-state currents were observed within experimental error.

All transient signals could be fit well (R^2 coefficient ~ 0.96 – 0.99) with a single purely exponential decay. Our observed results of the decay time τ as a function of inverse temperature and applied field are shown in Figures 2–5. The notation, M1 and M2, is used to distinguish two different crystals grown under approximately the same conditions. Subscripts a, b, etc. refer to different samples taken from a particular crystal.

Figures 2–5 demonstrate that in all cases the observed decay time exhibited an activated behavior. Figures 2 and 3 show the typical variation of activation energies within a particular crystal. The activa-

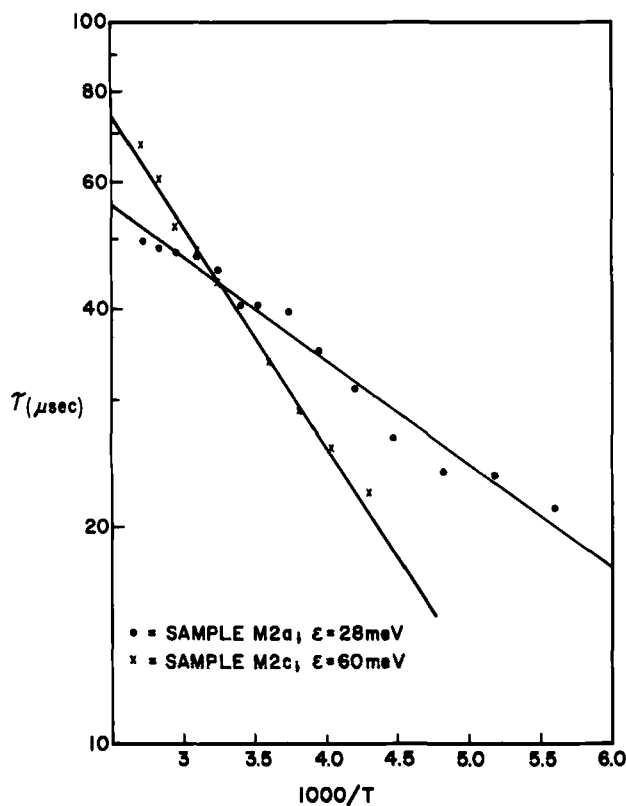


FIGURE 3 Electron trapping lifetime in anthracene (c' direction) versus inverse temperature for two samples from crystal M2. The applied field is $0.24 \text{ V}/\mu\text{m}$ for sample M2a and $0.32 \text{ V}/\mu\text{m}$ for sample M2c. ϵ is the activation energy.

tion energies varied from 30 to 84 meV, indicating that the observed behavior is extrinsic in nature. These data were repeatable upon temperature cycling. Figure 4 shows data over a wider temperature range for two different applied fields. Finally, $\tau(T)$ is plotted in Figure 5 for a wide range of temperatures (81–374 K) and fields (0.10–4.73 V/ μ m). The data may be fit with a single activation energy, indicating that the activation energy is not dependent on the applied field within experimental error. The data are summarized in Table I.

Another very important observation (not shown) is that the electron mobility, calculated from the observed transit time, is nearly independent of temperature ($\mu_e \sim T^{0.1}$) for all samples reported here. This

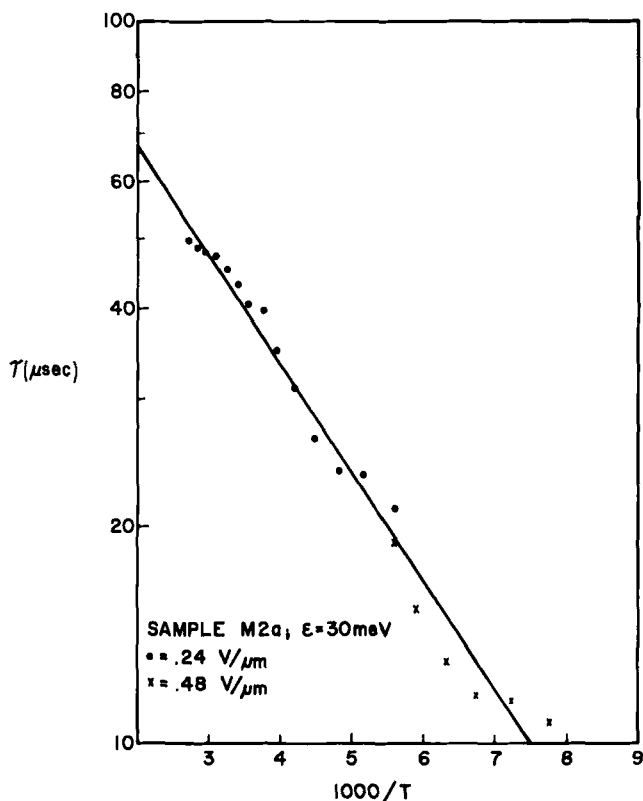


FIGURE 4 Trapping lifetime versus inverse temperature for two different applied fields, 0.24 and 0.48 V/ μ m, over an extended temperature range. ϵ is the activation energy.

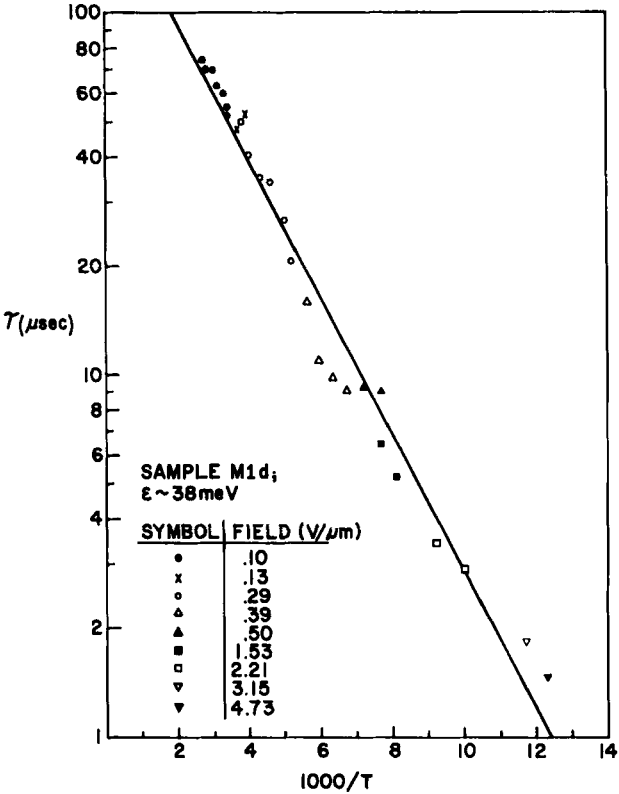


FIGURE 5 Trapping lifetime versus inverse temperature for a wide range of temperatures and applied fields, indicating the invariance of the activation energy ϵ .

TABLE I

Summary of $\tau(T)$ Results

Sample	Field ($\text{V}/\mu\text{m}$)	Temp. Range (K)	ϵ (meV)
M1a	0.20	213–374	57
M1b	0.20	222–374	68
M1c	0.18	234–374	84
M1d	0.10–4.70	81–374	38
M2a	0.24–0.48	130–370	30
M2b	0.26	190–370	46
M2c	0.32	230–370	60

indicates that the transport is intrinsic in nature² (i.e., not shallow-trap controlled).

IV. DISCUSSION

A number of trapping models will be reviewed in terms of their ability to account for our experimental results. Within these models, based on the justifications given above, dark-injection, space-charge effects, and diffusion will be neglected. The effect of the diagonal and off-diagonal components of the mobility tensor on the apparent trapping time will also be discussed.

The simplest model that can be proposed is a collection of monoenergetic traps distributed randomly throughout the crystal.⁹ This model has had wide application in the study of impurities in molecular crystals, where in most cases crystals such as anthracene or naphthalene have been doped with a known concentration of the impurity of interest (i.e., perylene,⁸ acridine and phenazine,⁷ anthraquinone, anthrone, and naphthacene⁹). In the trap-free case, the ideal current response is

$$\begin{aligned} I(t) &= nev_{\text{drift}} & t \leq \tau_0 \\ &= 0 & t > \tau_0 \end{aligned} \quad (1)$$

where n is the number of photogenerated charges, e is the electronic charge, v_{drift} is the drift velocity in the presence of an electric field, and τ_0 is the intrinsic transit time given by $\tau_0 = L^2/\mu V$, where L is the sample thickness, μ is the carrier mobility and V is the applied voltage. In the first approximation the effect of traps is to make n a time-dependent parameter, as it is only the free (mobile) carriers that contribute to the current. It is also assumed that the traps may be characterized by two trapping parameters, the average time τ_t between trapping events (the "trapping time") and the average time spent in a trap τ_d (the "detrapping time")^{9,10}:

$$\tau_t = (N_t \sigma v_{\text{max}})^{-1} \quad (2)$$

$$\tau_d = (N_c \sigma v_{\text{max}})^{-1} e^{\epsilon_t/kT} \quad (3)$$

where N_t is the trap density, σ is the trap capture cross-section, v_{max} is the maximum carrier velocity, N_c is the conduction band density of states, and ϵ_t is the trap depth (relative to the conduction band edge).

The pre-exponential factor in the definition of τ_d comes from detailed balance arguments.²⁷

The differential equations connecting the free-carrier population $n(t)$ with the trapped-carrier population $n_t(t)$ (for times shorter than the transit time) are

$$n + n_t = n_0 \quad (4)$$

$$\partial n(x, t)/\partial t = n(x, t)/\tau_t - n_t(x, t)/\tau_d \quad (5)$$

where n_0 is the number of photogenerated charges at $t = 0$. For times beyond the transit time the loss of carriers to the external circuit must be taken into account, and the solution does not have an analytical form.²⁸ The above equations are easily solved, and the current observed is proportional to the number of free carriers:

$$I(t) \propto n(t) = n_0/(\tau_d + \tau_t) \{ \tau_t + \tau_d \exp[-(\tau_d^{-1} + \tau_t^{-1})t] \}. \quad (6)$$

Care must be taken in properly defining the effective carrier mobility. In the cases of interest here the trapping time τ_t is much smaller than the intrinsic transit time τ_0 (in the opposite limit of $\tau_0 \ll \tau_t$ trapping events do not occur during a transit and trap information is not obtained). The mobility is modified because the effective transit time is now the sum of the intrinsic transit time plus the average amount of time that carriers spent in traps:

$$\tau_{\text{eff}} = \tau_0 + N\tau_d = \tau_0 + (\tau_0/\tau_t)\tau_d = \tau_0(1 + \tau_d/\tau_t) \quad (7)$$

where N is the average number of trapping events (τ_0/τ_t). This gives an effective mobility μ_{eff} of

$$\mu_{\text{eff}} = \mu_0(1 + \tau_d/\tau_t)^{-1} \quad (8)$$

where μ_0 is the intrinsic mobility.

Three different transport regimes may be defined. At high temperatures, defined by $\tau_d/\tau_t \ll 1$, we have $n(t) = n_0$ and $\mu_{\text{eff}} = \mu_0$. Trapped carriers are immediately released and trapping has little effect on the current and mobility. At intermediate temperatures, defined by $\tau_d/\tau_t \geq 1$, the familiar shallow trap controlled mobility model is obtained which predicts: i) the mobility is activated, ii) the current is the sum of a constant term plus a decaying exponential, and iii) the explicit temperature dependence of the decay time in the exponential term of the current (Eq. 6) *decreases* with increasing temperature. We have

observed a temperature-independent mobility, no indication of a steady-state current, and an exponential decay time that *increases* with increasing temperature. Clearly, this model in this temperature regime cannot account for our results. Finally, in the low-temperature regime defined by $\tau_d/\tau_t \gg 1$ the deep trap model is obtained. Specifically, with $\tau_t < \tau_0$ and $\tau_d \gg \tau_0$ free carriers are trapped and are not released on the time scale of the experiment. The current will be a pure decaying exponential with time constant $\tau = \tau_t$. No "kink" or transit time is observed because no carriers reach the rear electrode; all are trapped within the bulk of the crystal. The effective mobility, if it can be defined in such a case, is identically zero (Eq. (8) is still valid). (However, under conditions in which $\tau_0 \leq \tau_t$, there is a finite probability that some carriers will reach the other side of the sample, an effect ignored in Eqs. 4–6. In this case, a small kink may be observed in the current determined by the intrinsic mobility.²⁸)

In the applications of this single-trap model to date in anthracene the terms contributing to τ_t in Eq. (2) have been assumed to be, at most, weak functions of temperature.^{6–10} More will be said about this assumption later.

The next step in increasing complexity of trapping models is to consider the possibility of several sets of discrete traps, each of a different depth. The simplest example of such a model is one shallow trap and one deep trap, with k_{st} = shallow trap rate (the inverse of the trapping time), k_{sr} = shallow release rate (the inverse of the detrapping time), and k_{dt} = deep trap rate. The two traps in this example are "in parallel", meaning that there is no direct transition of an electron possible between them. In this case the differential equations coupling the free carrier population $n_f(t)$, the shallow trap population $n_s(t)$, and the deep trap population $n_d(t)$ are:

$$\partial n_f(t)/\partial t = -n_f(t)k_{st} - n_f(t)k_{dt} + n_s(t)k_{sr} \quad (9)$$

$$\partial n_s(t)/\partial t = -n_s(t)k_{sr} + n_f(t)k_{st} \quad (10)$$

$$\partial n_d(t)/\partial t = n_f(t)k_{dt} \quad (11)$$

The solution of these equations in terms of the free carrier population is

$$\begin{aligned} n_f(t) = n_0/2\alpha \{ & (k_{sr} - k_{st} - k_{dt} + \alpha)\exp[(\alpha - \beta)t/2] \\ & + (k_{dt} + k_{st} - k_{sr} + \alpha)\exp[-(\alpha + \beta)t/2] \} \\ \alpha \equiv & (\beta^2 - 4k_{sr}k_{dt})^{1/2}; \quad \beta \equiv (k_{st} + k_{sr} + k_{dt}) \end{aligned} \quad (12)$$

This model is interesting for the following reasons: the shallow trap is ineffective at high temperatures ($k_{sr} \gg k_{st}$) and only the deep trap contributes to the current decay; i.e., $I(t) \sim \exp(-k_{dt}t)$. At low temperatures ($k_{sr} \ll k_{st}$) the shallow trap becomes a deep trap and $I(t) \sim \exp[-(k_{dt} + k_{st})t]$. Theoretically, the current decays with a shorter time constant at lower temperatures, which qualitatively agrees with our $\tau(T)$ data. However, the model also makes a prediction for the observed mobility. As seen in the previous paragraph, deep traps do not contribute to the mobility and shallow traps contribute according to Eq. (8), which in this case may be written as

$$\mu_{eff} = \mu_0(1 + k_{st}/k_{sr})^{-1} \quad (13)$$

The effective mobility and the time dependence of the current are strongly coupled through the term k_{st}/k_{sr} . We observe (see Figure 5) an exponentially decaying current whose decay time constant varies smoothly by two orders of magnitude over a wide temperature range. The model predicts that this should be accompanied by a similar behavior in the observed mobility; i.e., the mobility is expected to vary by a large factor over our experimental temperature range to satisfy the inequalities, $k_{sr} \gg k_{st}$ at high temperatures and $k_{sr} \ll k_{st}$ at low temperatures. The model also predicts that the general form for the current in the intermediate temperature range is the sum of two decaying exponentials. Both of these predictions are inconsistent with our results.

The model is easily extended to include several independent discrete traps. In general, each new trap introduces an additional exponential term into the current and an additional ratio k_{tj}/k_{rj} into the expression for the effective mobility

$$I(t) \sim n_0 \sum_j A_j e^{-k_j t} \quad (14)$$

$$\mu_{eff} = \mu_0 \left\{ 1 + \sum_j k_{tj}/k_{rj} \right\}^{-1} \quad (15)$$

where the k_{tj} 's and k_{rj} 's are the trapping and release rates for the j^{th} discrete trap and the A_j 's and k_j 's are convolutions of these rates. The model predicts currents which are the sum of exponential terms and effective mobilities which are, in general, dependent on temperature. These predictions are contrary to our results.

In a recent paper on exciton transport in tetracene-doped anthracene, Braun, *et al.*²⁹ invoked shallow "pre-traps" in the vicinity of the

tetracene molecules (deep traps) in order to account for the observed temperature dependence of the exciton transfer rate. Such a model, identical with the two-trap model described above with the traps in series rather than in parallel with each other, may account for our data. The differential equations connecting the free-carrier population $n_f(t)$, the shallow-trap population $n_s(t)$, and the deep-trap population $n_d(t)$ are:

$$\partial n_f(t)/\partial t = -n_f(t)k_{st} + n_s(t)k_{sr} \quad (16)$$

$$\partial n_s(t)/\partial t = n_f(t)k_{st} - n_s(t)k_{sr} - n_s(t)k_{sd} \quad (17)$$

$$\partial n_d(t)/\partial t = n_s(t)k_{sd} \quad (18)$$

where k_{st} is the shallow trapping rate, k_{sr} is the shallow release rate, and k_{sd} is the transfer rate from the shallow to the deep traps. Equations of this type are common in chemical kinetics problems, and their solutions are well known.³⁰⁻³² The free-carrier solution is³⁰

$$\begin{aligned} n_f(t) = n_0/2\alpha \{ & (k_{sr} + k_{sd} - k_{st} + \alpha)\exp[(\alpha - \beta)t/2] \\ & + (k_{st} - k_{sd} - k_{sr} + \alpha)\exp[-(\alpha + \beta)t/2] \} \\ \alpha \equiv & (\beta^2 - 4k_{st}k_{sd})^{1/2}; \quad \beta \equiv (k_{st} + k_{sr} + k_{sd}) \end{aligned} \quad (19)$$

In general, the presence of the shallow trap will induce an activated behavior in the effective mobility (e.g. Eq. 13). In order for the predictions of this model to be consistent with our experimental results (temperature-independent mobility), we confine our considerations to the case of $k_{st} \ll k_{sr}$ for all temperatures of experimental interest. Free carriers will come into quasi-equilibrium with the shallow traps after a time $\tau_{\text{equil}} = (k_{st} + k_{sr})^{-1}$ (see Eq. 6). For times $t \gg \tau_{\text{equil}}$, the first exponential term in Eq. 19 will dominate the decay, and the decay rate may be approximated by a truncated binomial expansion:

$$\begin{aligned} (\alpha - \beta)/2 \approx & (k_{st} + k_{sd})/(k_{st} + k_{sr} + k_{sd}) \\ & + (k_{st} + k_{sd})^2/(k_{st} + k_{sr} + k_{sd})^3 \cdots \end{aligned} \quad (20)$$

The necessary condition for the first term to adequately represent the series is that $4k_{st}k_{sd}/(k_{st} + k_{sr} + k_{sd})^2$ be small compared to one, which is true when $k_{st} \ll k_{sr}$. If we further restrict our considerations to the case of $k_{sd} \ll k_{sr}$, and retain only the first term in the binomial

expansion, then Eq. 19 simplifies to

$$n_f(t) \approx n_0 \exp(-Kt) \quad (21)$$

$$K \equiv k_{st}k_{sd}/k_{sr} = N_s(N_c N_d \sigma_d v_{\max})^{-1} e^{\epsilon_s/kT} \quad (22)$$

where N_s is the shallow trap density, N_c is the conduction band density of states, N_d is the deep trap density, σ_d is the deep trap capture cross-section, v_{\max} is the maximum velocity, and ϵ_s is the shallow trap depth. This model predicts a deactivated decay rate for the current and a temperature-independent mobility. Both of these predictions are in agreement with our experimental results. According to Eq. 22, the observed activation energy is to be identified with the depth of the shallow trap. In the previous section we noted that observed activation energies varied widely from sample to sample for any particular crystal. It is not clear to the authors how known shallow trapping mechanisms could account for this wide variation of apparent trap depths among samples. This model also requires a strong association between the shallow and deep traps, suggesting that they are in the same vicinity. Such a configuration might result from lattice distortions in the neighborhood of an impurity or dislocation, or the shallow traps may correspond to vibronic levels of an impurity molecule.²⁹

It has been suggested that the field and temperature dependence of the transient current in anthracene can be explained by a dispersive transport model.³³ Such a model assumes a continuous distribution of traps in the band gap with the exact form of the distribution being somewhat arbitrary. The theory was originally worked out by Scher and Montroll³⁴ for hopping transport with a wide range of hopping times, and has been shown to be formally equivalent to the case of band transport with a wide range of trap-release times.³⁵ The theory has been successfully applied to explain transport in a number of amorphous semiconductors.³⁶⁻³⁹ If an exponential trap distribution of the form $g_{\text{trap}}(\epsilon) = N_t \exp(-\epsilon/kT_0)$ is assumed, the theory predicts

$$\begin{aligned} I(t) &\propto t^{-(1-\alpha)} & t < \tau' \\ &\propto t^{-(1+\alpha)} & t > \tau' \end{aligned} \quad (23)$$

$$\mu' \propto (E/L)^{(1/\alpha-1)} \sim e^{-\epsilon_a/kT}; \quad \epsilon_a = kT_0 \ln [L(2\mu_0 E \tau_i)^{-1/2}] \quad (24)$$

where τ' is the effective transit time, μ' is the corresponding effective

mobility, and $\alpha = T/T_0$ is the dispersion parameter. Our transient currents may be fitted reasonably well with a power-law decay, and the resulting power is linear in temperature, confirming the first prediction. However, we have seen no evidence of a field⁴⁰ or temperature dependent mobility, indicating that this model is not appropriate for transport in crystalline anthracene.

We have calculated the effect of the anisotropy of the diagonal components of the mobility tensor in anthracene on the apparent electron trapping lifetime. In the *ab* plane, the mobility increases with decreasing temperature, i.e., $\mu_a \sim T^{-1.6}$ and $\mu_b \sim T^{-0.84}$, while the mobility in the *c'* direction remains nearly independent of temperature.⁵ If the off-diagonal components of the mobility tensor are ignored (these will be discussed below), then it can be assumed that with the electric field in the *c'* direction (perpendicular to the *ab* plane) there are no electric field components in the *ab* plane and hence no contributions from drift velocity in that plane. Hence, any velocity components in the plane are diffusional. Diffusion has been neglected until now, but as noted above, the mobilities in the *ab* plane at low temperatures can be quite high and hence two-dimensional diffusion in that plane may be significant. The diffusion constant is connected to the mobility through the Einstein relation $\mu = eD/kT$. This then is the picture we present: at high temperatures the diffusion constants in all directions are small and diffusion may be neglected. At low temperatures, μ_a and μ_b have increased significantly and therefore a free charge packet suffers diffusional spreading in the *ab* plane. With this spreading out of the charge packet at lower temperatures, the electrons encounter more lattice sites and hence more trapping sites, which would be observed experimentally as an increase in the trapping efficiency (i.e., shorter trapping time). The magnitude of this effect may be calculated as follows: we have calculated the average trapping time based on a three-dimensional anisotropic hopping model with deep traps. The function of primary interest is the number of new sites sampled as a function of time. If we assume for simplicity that the mobility is isotropic in the *ab* plane, then this function has the form⁴¹

$$S(t) = (4\pi W_{ab}t)/\log[32W_{ab}/W_{c'}] \quad (25)$$

where W = hopping rate $= \mu kT/ea^2$ (a is the lattice constant). The probability that a free electron will become trapped when it encounters a new site is $c = N_t/N_c$, the molar concentration of traps. Hence the total probability that a free electron will be trapped is $P_t(t) = cS(t)$. The average trapping time is defined as the time it takes for this

probability to reach unity. Therefore

$$cS(t = \tau) = 1 \rightarrow \tau = c \log[32W_{ab}/W_{c'}]/4\pi W_{ab} \quad (26)$$

$$\therefore \tau \sim T^{0.6} \log(T^{1.7}) \quad (27)$$

where we have made use of the Einstein relation and have assumed $\mu_{\perp c'} = \mu_{aa}$ so that Eq. (27) represents the strongest possible temperature dependence of τ . If the data in Figure 5 is replotted log-log, then the activated behavior of τ may also be interpreted as a power-law behavior with $\tau \sim T^{2.6}$. Although this model can account for a temperature independent c' mobility and simultaneously a trapping time that increases with temperature, clearly the strong temperature dependence of τ that we observe cannot be accounted for.

We have also considered the contribution of the off-diagonal component of the anthracene mobility tensor to the apparent trapping time, which may be significant at low temperatures.^{42,43} According to the experimental results of Karl,⁴² $\mu_{ac'}$ is approximately zero at room temperature, but its magnitude increases to nearly that of the diagonal c' component at 150 K (μ_{ab} and $\mu_{bc'}$ are zero at all temperatures because b is a principal axis of the crystal). In other words, with an electric field in the c' direction the drift velocity vector points along the c' direction at room temperature. At 150 K, however, the c' component has changed very little, but a new velocity component v_a along the a direction has been added. In a sandwich configuration with the electrodes parallel with ab and E parallel with c' , the electrons will drift *diagonally* across the sample. If we assume that the velocity v_{\max} in Eq. (2) for the trapping time is the magnitude of the drift velocity, then we can calculate qualitatively the relative change in τ_t due to the increase in $v_{\text{drift}} = v_{c'} + v_a(T)$ at lower temperatures. Using Karl's results [$\mu_{c'c'}(300 \text{ K}) = 0.39$, $\mu_{c'c'}(150 \text{ K}) = 0.35$, $\mu_{c'a}(300 \text{ K}) \sim 0$, $\mu_{c'a}(150 \text{ K}) = 0.32 \text{ cm}^2/\text{V sec}$],⁴² we have

$$v_{\text{drift}} = \mu_{c'c'} E c' + \mu_{c'a} E a \quad (28)$$

which gives

$$|v_{\text{drift}}| = [(\mu_{c'c'})^2 + (\mu_{c'a})^2]^{1/2} E \quad (29)$$

where a is a unit vector in the a direction and c' is the unit vector in the c' direction, and we have assumed that the trap density and capture cross-section are independent of temperature. Using Karl's numbers,

we obtain $\tau_r(150 \text{ K})/\tau_r(300 \text{ K}) = v_{\text{drift}}(300 \text{ K})/v_{\text{drift}}(150 \text{ K}) = \{[(0.35)^2 + (0.32)^2]^{1/2} E\}/(0.39)E = 0.83$. We see that the change in the apparent trapping efficiency due to the off-diagonal contribution of the mobility tensor is only $\sim 17\%$ from 300 K to 150 K, much too small a change to account for our results.

Finally, we must return to the question of whether or not the other factors contributing to τ_r in Eq. (2) may themselves be temperature dependent. The strongest possible temperature dependence in v_{max} is accounted for if we assume it is the thermal velocity. The thermal velocity may have at most a $T^{1/2}$ behavior if one invokes the equipartition theorem, and this dependence obviously has the wrong sign and is not strong enough to account for our data.

A trap density that decreases in a reversible way with increasing temperature does not seem reasonable to the authors. Point defects are equilibrium imperfections and their density increases with temperature.⁴⁴ Point defects created during crystal growth might anneal, but their concentration is not reversible with temperature. Dislocations are introduced during solidification of the crystal from the melt and their density may be significantly reduced by annealing.⁴⁵ Our $\tau(T)$ data was recorded beginning at high temperatures and hence the dislocation densities present were minimized. We have considered the possibility that our experimental configuration (brass spring-loaded plunger pressing the crystal against Nesa-coated quartz) may be exposing the crystals to an external temperature dependent strain. The experiments have been repeated using an absolute minimum of physical contact between the brass plunger and the crystals. An identical strong temperature dependence of the apparent trapping time was observed, discounting this hypothesis. Qualitatively similar results were obtained with sublimation flakes (in which dislocations are believed to be significantly reduced).

A temperature dependent trap capture cross-section is an interesting possibility. Within the realm of the more familiar (and correspondingly better understood) semiconductors a number of mechanisms have been used to explain observed temperature-dependent trapping lifetimes. O, Cu, Fe, and Cr impurities in GaAs have been studied and the process of multi-phonon emission has been invoked to yield $\sigma \sim \exp(-\epsilon_a/kT)$, i.e., a cross-section that increases rapidly with temperature.⁴⁶ Although the sign of the exponent does not agree with our results, the example is useful in demonstrating an established mechanism for a temperature dependent cross-section. Another example is the phonon cascade process, which explains trapping lifetimes that increase rapidly with temperature in the case of As and Sb

impurities in Ge.⁴⁷ This trap model depends on the trap being represented by a long-range attractive potential well, with many discrete levels within the well, which is easily justified for a positively charged trap, less easily for a neutral trap, and not at all for a negatively charged trap^{48,49} (assuming electron trapping). In our experiments, the electrodes were grounded between transients and the crystal exposed to several laser pulses in order to neutralize trapped charge. On the first of such shots after a recorded electron transient, we always observed a positive, quickly decaying current. This indicated that the trapped electrons created their own self-induced field, attracting free holes created by the laser pulse. We conclude that the empty traps were neutral, while the filled traps were negatively charged by the electrons residing in them. Most known neutral trap mechanisms cannot be represented by a long-range potential and have only a few excited states at most. Therefore, we conclude that the phonon cascade process is not operative in our experiment.

A deep trap with associated shallow “pre-trap” model, or a single trap level with a temperature dependent cross-section are the most promising directions that the authors can suggest for a possible explanation of our results. We note the need for more work on the development of trapping theories, the understanding of trapping mechanisms, and the interaction of these mechanisms with the unique transport properties characteristic of organic semiconductors.

V. CONCLUSIONS

We have presented data for the electron trapping lifetime in the *c'* direction of anthracene over a wide range of temperatures and applied electric fields. We conclude that the trapping lifetime is activated and that the activation energy is independent of applied field (0.10–4.73 V/ μm) and temperature (81–374 K). The variation in the activation energy from sample to sample (30–84 meV) indicates that the trapping is an extrinsic process.

We have considered several trapping models and have compared predictions of these models with our results. A system of parallel discrete traps with temperature independent densities and cross-sections cannot account for our results. A model consisting of a shallow “pre-trap” in series with a deep trap, under the constraints that the trapping rate into the shallow trap and the transfer rate from shallow to deep trap are much smaller than the detrapping rate from the shallow trap to the conduction band at all temperatures of interest,

predicts a temperature independent mobility and a temperature activated effective trapping time constant, which is consistent with our results. It is not clear what trapping mechanisms in such a model could account for the wide range of activation energies that we have observed. A continuous distribution of traps can account for the temperature dependence of the lifetime that we observe, but the field and temperature dependent mobility predicted by this model have not been observed. We have considered the effect of the anisotropy of the diagonal mobility components, as well as the contribution of the off-diagonal components to the apparent trapping efficiency in anthracene. Either of these effects can qualitatively explain both our $\mu(T)$ and $\tau(T)$ data, but cannot quantitatively account for the strong temperature dependence of $\tau(T)$. We note that a temperature dependent trapping cross-section may play a role in our experiment, and we recognize the need for the development of specific trapping mechanisms that take into account the band structure, lattice structures, and phonon interactions peculiar to organic semiconductors.

Acknowledgments

The authors would like to thank H. Scher, W. Johnson, R. Young and V. Kenkre for many helpful discussions, and R. Markham for technical assistance. This work was supported in part by the NSF Materials Research Laboratory under grant #DMR7923647.

References

1. L. B. Schein and A. R. McGhie, *Phys. Rev. B*, **20**, 1631 (1979).
2. L. B. Schein, *Chem. Phys. Lett.*, **48**, 571 (1977).
3. P. S. Vincent, W. A. Barlow, R. A. Hann and G. G. Roberts, *Thin Solid Films*, **94**, 171 (1982).
4. J. Dresner, *RCA Rev.*, **30**, 322 (1969).
5. L. B. Schein and D. W. Brown, *Mol. Cryst. Liq. Cryst.*, **87**, 1 (1982).
6. K. Oyama and I. Nakada, *J. Phys. Soc. Jpn.*, **24**, 792 (1968).
7. K. H. Probst and N. Karl, *Phys. Stat. Sol.*, **27a**, 499 (1975).
8. M. Samoc, *Mol. Cryst. Liq. Cryst. Lett.*, **34**, 171 (1977).
9. D. C. Hoesterey and G. M. Letson, *J. Phys. Chem. Sol.*, **24**, 1609 (1963).
10. T. Garofano, *IL Nuovo Cimento*, **21B**, 376 (1974).
11. M. Samoc and Z. Zboinski, *Phys. Stat. Sol.*, **46a**, 251 (1978).
12. F. C. Aris, T. J. Lewis, J. M. Thomas, J. O. Williams and D. F. Williams, *S. S. Comm.*, **12**, 913 (1973).
13. P. J. Reucroft and F. D. Mullins, *Mol. Cryst. Liq. Cryst.*, **23**, 179 (1973).
14. M. Gamoudi, N. Rosenberg, G. Guillard, M. Maitrot and G. Mesnard, *J. Phys. C*, **7**, 1149 (1974).
15. M. Samoc, A. Samoc, J. Sworakowski and N. Karl, *J. Phys. C*, **16**, 171 (1983).

16. T. Garofano, T. Corazzani, and G. Casolini, *IL Nuovo Cimento*, **38B**, 133, 141 (1977).
17. G. M. Parkinson, J. M. Thomas and J. O. Williams, *J. Phys. C*, **7**, L310 (1974).
18. G. Dietrich, H. Pick, and H. Bauser, *Chem. Phys. Lett.*, **33**, 257 (1975).
19. P. Mark and W. Helfrich, *J. Appl. Phys.*, **38**, 205 (1962).
20. E. A. Silinsh, *Proceedings of the International Conference on Defects in Crystals*, Riga, May, 1981, (Springer-Verlag, Heidelberg, 1982).
21. J. Sworakowski, *Mol. Cryst. Liq. Cryst.*, **11**, 1 (1970); **33**, 83 (1976).
22. R. W. Munn, *Mol. Cryst. Liq. Cryst.*, **31**, 105 (1975).
23. S. Nespurek and E. A. Silinsh, *Phys. Stat. Sol.*, **34a**, 747 (1976).
24. S. Z. Weisz, A. Cobas, S. Trester and A. Many, *J. Appl. Phys.*, **39**, 2296 (1968).
25. N. Karl, *Z. Naturforsch.*, **259**, 382 (1970).
26. L. B. Schein, R. W. Anderson, R. C. Enck and A. R. McGhie, *J. Chem. Phys.*, **71**, 3189 (1979).
27. W. Shockley and W. T. Read, *Phys. Rev.*, **87**, 835 (1952).
28. W. E. Tefft, *J. Appl. Phys.*, **38**, 5265 (1967).
29. A. Braun, U. Mayer, H. Auweter, H. C. Wolf and D. Schmid, *Z. Naturforsch.*, **37a**, 1013 (1982).
30. T. Lowry and W. John, *J. Chem. Soc. London*, **97**, 2634 (1910).
31. D. McDaniel and C. Smoot, *J. Phys. Chem.*, **60**, 966 (1956).
32. C. Bamford and C. Tipper, eds., *Comprehensive Chemical Kinetics*, vol. 2, Elsevier Publishing Company, New York, 1969.
33. J. B. Webb, D. F. Williams and J. Noolandi, *S. S. Comm.*, **31**, 905 (1979).
34. H. Scher and E. W. Montroll, *Phys. Rev. B*, **12**, 2455 (1975).
35. J. Noolandi, *Phys. Rev. B*, **16**, 4466 (1977).
36. G. Pfister and H. Scher, *Phys. Rev. B*, **15**, 2062 (1977).
37. B. A. Kahn, M. A. Castner and D. Adler, *S. S. Comm.*, **45**, 187 (1983).
38. G. Pfister, *Phys. Rev. Lett.*, **36**, 271 (1976).
39. V. I. Arkhipov, M. S. Iovu, A. I. Rudenko and S. D. Shutov, *Phys. Stat. Sol.*, **54a**, 67 (1979).
40. L. B. Schein, R. S. Narang, R. W. Anderson, K. E. Meyer and A. R. McGhie, *Chem. Phys. Lett.*, to be published.
41. H. Scher, S. Alexander and E. Montroll, *Proc. Natl. Acad. Sci., USA*, **77**, 3758 (1980).
42. N. Karl, *Proceedings of the Ninth Molecular Crystal Symposium*, Mettelberg, Kleinwalsertal, p. 149 (1980).
43. E. Irene, P. Walker, A. P. Marchetti and R. H. Young, *J. Chem. Phys.*, **68**, 4134 (1978).
44. E. A. Silinsh, *Organic Molecular Crystals*, Springer-Verlag, Berlin, 1980 (p. 154).
45. M. Pope and C. E. Swenberg, *Electronic Processes in Organic Crystals*, Oxford University Press, New York, 1982 (p. 227).
46. C. H. Henry and D. V. Lang, *Phys. Rev. B*, **15**, 989 (1977).
47. G. Ascarelli and S. Rodriguez, *Phys. Rev.*, **124**, 1321 (1961).
48. V. L. Bonch-Bruевич and E. G. Landsberg, *Phys. Stat. Sol.*, **29**, 9 (1968).
49. P. T. Landsberg, *Phys. Stat. Sol.*, **41**, 457 (1970).